
SOLVING THE REAL-TIME TRAIN DISPATCHING PROBLEM BY COLUMN GENERATION

 **Maik Schälicke** *

Dresden University of Technology
Chair of Traffic Flow Science

Hettnerstraße 1, 01069 Dresden, Germany

<https://tu-dresden.de/bu/verkehr/ila/vkstrl>

Karl Nachtigall

Dresden University of Technology
Chair of Traffic Flow Science

Hettnerstraße 1, 01069 Dresden, Germany

January 22, 2024

ABSTRACT

Disruptions in the operational flow of rail traffic can lead to conflicts between train movements, such that a scheduled timetable can no longer be realised. This is where dispatching is applied, existing conflicts are resolved and a dispatching timetable is provided. In the process, train paths are varied in their spatio-temporal course. This is called the train dispatching problem (TDP), which consists of selecting conflict-free train paths with minimum delay. Starting from a path-oriented formulation of the TDP, a binary linear decision model is introduced. For each possible train path, a binary decision variable indicates whether the train path is used by the request or not. Such a train path is constructed from a set of predefined path parts (speed-profiles) within a time-space network. Instead of modelling pairwise conflicts, stronger MIP formulations are achieved by cliques formulated over the complete train path. The combinatorics of speed-profiles and different departure times results in a large number of possible train paths, so that the column generation method is used here. Within the subproblem, the shadow prices of conflict cliques must be taken into account. When constructing a new train path, it must be determined whether this train path belongs to a clique or not. This problem is tackled by a MIP. The methodology is tested on instances from a dispatching area in Germany. Numerical results show that the presented method achieves acceptable computation times with good solution quality while meeting the requirements for real-time dispatching.

Keywords Train Dispatching · Column Generation · Speed Profiles

1 Introduction to the TDP

In railway operations, train dispatching stands as one of the most crucial and challenging tasks. In the event of operational disruptions, it may become impossible to execute the planned operational schedule. In such instances, dispatchers must contribute to achieving the dispatching objective: the fastest possible return to the planned and conflict-free timetable. Considering all involved train services and the available infrastructure, this poses an exceedingly complex task. To manage the dispatcher workload, they are responsible for a spatially delimited area known as the dispatching area. Moreover, only train services within a temporally dispatching horizon are considered. Within this spatially and temporally delimited area, dispatchers employ dispatching measures such as rerouting or rescheduling to achieve the dispatching objective. By applying these measures, they aim to optimize network capacity utilization to minimize delays for train services. Hence, a train service seeks a conflict-free train path with minimal delays. Thus, the Train Dispatching Problem (TDP) can be defined as the conflict-free selection of train paths for the set of train services within the dispatching area and horizon, aiming to minimize delays.

To further aid dispatchers in solving the TDP, computer-assisted methods are employed. This paper introduces an algorithmic approach to solve the TDP. Section 2 provides a brief overview of existing approaches. The subsequent

*maik.schaelicke1@tu-dresden.de

Section 3 details the approach presented in this study. Numerical computations and their results are presented in Section 4. Finally, a concise summary and outlook are provided (Sect. 5).

2 Related Research and This Work

According to [Fang et al. \(2015\)](#), alternative graphs (AG) ([Mascis and Pacciarelli, 2002](#)) are widely applied, particularly for conflict resolution. In the context of real-time train dispatching, [D’Ariano et al. \(2007\)](#) utilise an AG-based formulation. In this approach, the routes are fixed, and the selection of arcs from pairwise incompatible arcs represents a valid scheduling or sequence of trains. To solve their AG model, [D’Ariano et al.](#) present a branch-and-bound algorithm. In a subsequent work, the real-time traffic management system ROMA (Railway Traffic Optimization by Means of Alternative Graphs) is introduced ([D’Ariano et al., 2008](#)). The model from [D’Ariano et al. \(2007\)](#) is extended to include train routing, using a local search algorithm. For routing and scheduling, [Corman et al. \(2010\)](#) present a tabu search algorithm. In [Samà et al. \(2017\)](#), different strategies for exploring neighbourhoods are examined and compared with the local search by [D’Ariano et al. \(2008\)](#) and the tabu search algorithm by [Corman et al. \(2010\)](#). It has been shown that optimal solutions are only available for smaller instances ([Corman et al., 2010](#)), or at least, an advantage in terms of computation time can be achieved ([Samà et al., 2017](#)). However, the full potential of train routing cannot be fully realised through AG formulations ([D’Ariano et al., 2008](#)).

To overcome the limitations of AG, mixed-integer programming (MIP) formulations are employed, which find broad applications in real-time train scheduling and dispatching ([Fang et al., 2015](#)). In MIP formulations, the time at which a train traverses a track component of its selected route is expressed using a continuous variable. This necessitates disjunctive conditions to decide on the sequence in which trains traverse the track component, and linear constraints are formed using binary variables and big-M constraints. Conflict resolution is achieved explicitly by using minimum headway times based on the blocking time model ([Pachl, 2021](#), p. 26ff). [Pellegrini et al. \(2012\)](#) present a MIP that includes a detailed modelling of the infrastructure based on track circuits. Test instances within a dispatching area around Lille-Flandres station are optimally solved. In [Pellegrini et al. \(2014\)](#), the MIP is used within a rolling horizon approach. In a subsequent work by [Pellegrini et al. \(2015\)](#), a heuristic is introduced for these MIP formulations, allowing for high-quality solutions in real-time train dispatching in complex infrastructure areas. Providing high-quality solutions while meeting real-time requirements is one of the major challenges in real-time applications. Such a support system was applied in Norway, based on a decomposition approach by [Lamorgese and Mannino \(2012\)](#). [Lamorgese and Mannino](#) use a MIP formulation for real-time train dispatching and geographically divide the problem into a line problem and a station problem, reducing the number of big-M constraints. The line problem serves as the master problem, and the station problem forms the subproblem. Based on this decomposition, the solution is obtained similarly to Benders’ decomposition, by generating feasible cuts. In [Lamorgese et al. \(2016\)](#), a heuristic for this decomposition approach was presented, improving the speed of the solution process. Comprehensive overviews of MIP models for real-time train dispatching in railway operations can be found in the review articles by [Cacchiani et al. \(2014\)](#) and [Fang et al. \(2015\)](#).

The drawback of MIP models lies in their linear programming (LP) relaxation. This relaxation depends on the choice of big-M, but generally represents a weak formulation ([Lodi, 2010](#); [Bonami et al., 2015](#)). In contrast to disjunctive MIP models, time-index models ([Dyer and Wolsey, 1990](#)) discretise the time horizon into time intervals without the need for big-M constraints. The allocation of a track component to a discrete time interval represents a spatial-temporal resource utilisation. For a train path, a path within a space-time network represents an allocation of these resources. In an IP (integer programming) formulation, binary variables are used to decide on the utilisation of these spatial-temporal resources for individual trains. Conflict avoidance is guaranteed through set packing constraints for individual spatial-temporal resources. The critical point in time-index models is the discretisation into time intervals. Finer granularity in the time component results in a large number of binary variables. To manage this, decomposition techniques can be used by splitting the original problem into a master problem and multiple subproblems. This decomposition typically relates to trains. Independent subproblems, representing train-specific issues, can be formulated as a path-based problem ([Leutwiler and Corman, 2023](#)).

In the literature, decomposition approaches for time-index models are primarily found in the formulation of the Train Timetabling Problem (TTP). Similar approaches can be applied to the Train Dispatching Problem (TDP), as it is an online manifestation of the TTP. However, limitations arise due to the macroscopic perspective in the TTP. The basic idea behind decomposition is to formulate the feasibility conditions, i.e., the requirement for conflict avoidance, in a master problem. To achieve this, cliques of pairwise incompatible arcs in a space-time network, representing the utilized track components of a train path, are formed and expressed as set packing constraints in the integer programming (IP) formulation ([Brännlund et al., 1998](#); [Cacchiani et al., 2012](#)). [Caprara et al. \(2002\)](#), [Caprara et al. \(2006\)](#), and [Cacchiani et al. \(2008\)](#) formulate capacity constraints over the nodes of the space-time network instead of the arcs to reduce the number of constraints. Another approach is pursued in the works of [Borndörfer and Schlechte \(2007\)](#) and [Borndörfer](#)

et al. (2010), where feasible arc configurations are assigned to each train path, forming a feasible set of arcs, i.e., conflict free track components. In this approach, the focus is not on conflict exclusion but rather on selecting feasible routes. Depending on the formulation of the master problem, in all cases, train paths are generated in the subproblems, which are obtained by applying Lagrangian relaxation (Brännlund et al., 1998; Caprara et al., 2002, 2006; Cacchiani et al., 2012) or through column generation (CG) (Borndörfer and Schlechte, 2007; Borndörfer et al., 2010; Cacchiani et al., 2008).

In the context of real-time train dispatching, Lusby et al. (2013) present a path-based formulation. In an integer programming (IP) model, a binary variable is used to assign a train path to each train service. Lusby et al. consider three factors for possible paths: crossing opportunities, train kinematics, and the signal system. Considering these factors, all possible paths, i.e., train paths, are formulated in a tree structure. For track capacities, the spatial-temporal resources used by the path are considered. Using set packing formulations, each resource can be claimed by only one train service. The problem is decomposed similarly to column generation. However, unlike classical column generation, the subproblem is not formulated as an optimization problem. Instead, pricing and generating new train paths are done by recursively traversing the developed tree structure. A branch-and-price algorithm is used for generating integer solutions and evaluating their quality.

In Meng and Zhou (2014), a decomposition approach is applied to an edge-based IP. The capacity constraint is formulated for train pairs over individual track components. These constraints affect multiple trains and are identified as complicating constraints. Applying Lagrangian relaxation to these capacity constraints results in train-specific subproblems in the form of time-dependent shortest path problems. Meng and Zhou present a label-correcting algorithm for solving these subproblems.

In Bettinelli et al. (2017), the problem is divided into a construction phase and a shaking phase. In the construction phase, a train path is generated by solving a shortest path problem within a space-time network individually for each train service. In the shaking phase, the train order is varied while considering dispatching rules and conflicts. Bettinelli et al. use and compare a local search algorithm called reduced variable neighbourhood search and a tabu search for this purpose. The construction and shaking phases are iteratively executed to improve the solution.

For real-time train dispatching, Reynolds et al. (2020) and Reynolds and Maher (2022) use an edge-based IP. They restrict the simultaneous usage of track components in a way that they can be occupied or banned. The IP formulation of these capacity constraints is based on set packing conditions. Using Danzig-Wolfe decomposition, the authors transition from edge-based to path-based formulation and solve it using a branch-and-price algorithm. Subproblems can also be solved using shortest path algorithms in this approach.

For a comprehensive overview of decomposition approaches for railway scheduling problems, please refer to Leutwiler and Corman (2023).

In order to be able to react at any time online on modified traffic situations, the calculation time to solve the problems should be in the range of seconds. For these reasons, we do not determine the global optimum with a branch-and-price method, but only solve the relaxation with column generation from which an integer solution is determined at the end. By means of a Lagrange relaxation we can specify lower limits to the global optimum, which in many cases show a good quality of the calculated solution. Traditionally, column generation is aimed to solve the LP-relaxation as quickly as possible without any concern for the integer properties of the columns formed. In our approach, we aim to generate columns, which will forming a good integer solution. Instead of using pairwise conflict constraints, we will use maximum conflict cliques, which is a much stronger model formulation. Solving the pricing problem with maximum cliques as conflict restrictions is a big challenge, because optimizing a new train path must take all shadow prices of the cliques that contain this train path into account.

3 TDP Solution Algorithm

A train path $((v_1, t_{v_1}), \dots, (v_n, t_{v_n}))$ will be described by sequence of path segments (v_i, t_{v_i}) , so called speed-profiles v_i and time points t_{v_i} . A speed-profile v has only a temporal length, but no fixed time. Minimum headway times between train paths will be calculated from time points t_v and the minimum headway times between speed-profiles. The driving dynamic calculation of the speed-profiles and their minimum headway times are carried out as a preprocess and thus, strictly separated from the optimization core (Fig. 1).

This approach has the advantage, that the optimization is independent of the speed-profile construction process. Speed-profiles can be generated using commercial software such as LUKS (VIA-Con) or through custom-developed methods based on space-time networks (e.g. Lusby et al., 2013). The preprocessing part can occur in a more strategic planning manner, that means a set of speed-profiles can be generated beforehand and stored in a database. The database needs to be updated to reflect the current railway traffic situation.

The optimization core is a path-based formulation, where each train path for every train service is modelled by a binary decision variable. Conflict restrictions between train paths are formulated by maximum cliques. Due to the huge number of variables we will use a column generation algorithm (PMC-CG) to solve the TDP.

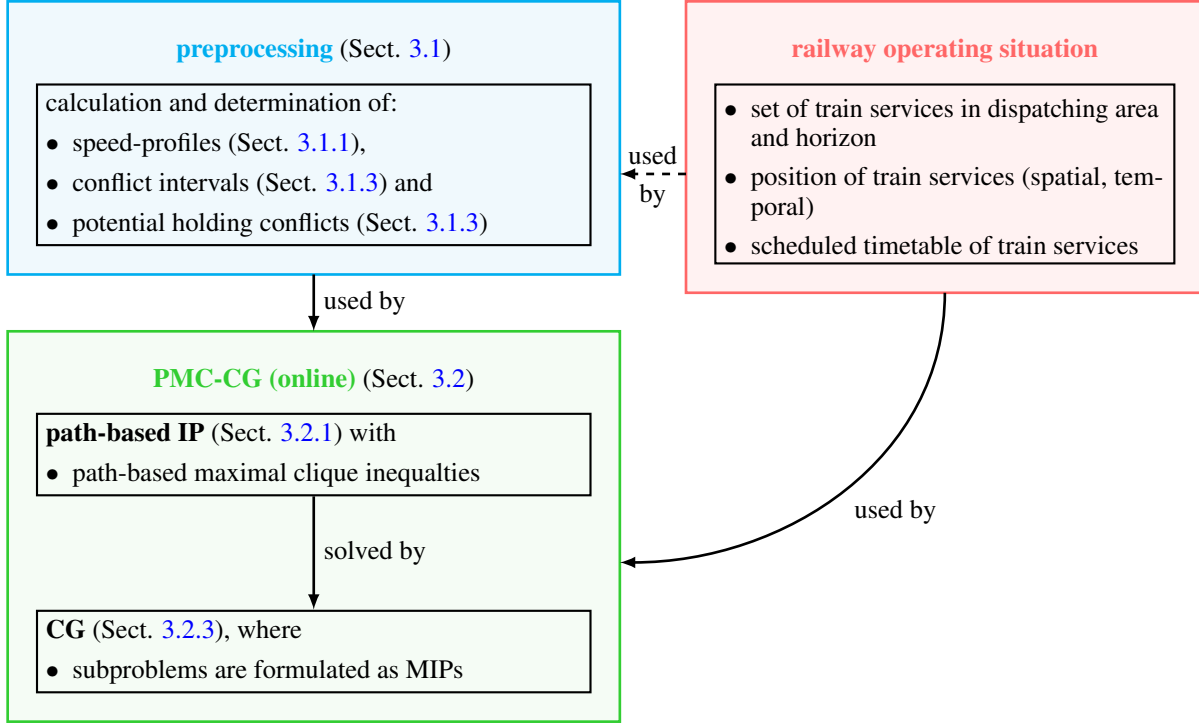


Figure 1: Two-part approach for the TDP with an independent real-time train dispatching algorithm decoupled from the train path generation.

3.1 Preprocessing

3.1.1 Speed-Profiles

The concept of speed-profiles corresponds to snippets described in [Nachtigall and Opitz \(2016\)](#) or [Dahms et al. \(2019\)](#), used for generating schedules for freight trains by providing train paths for these trains. Mathematically, a speed-profile represents a space-time function. The spatial extent for a speed-profile is limited by points where dispatching decisions can be made, referred to as dispatching points. The speed-profiles given by the preprocess define the potential of possible dispatching decisions. Regardless of the optimization, they can be designed from simple to arbitrarily complex.

For the sequence of block sections utilized by a speed-profile v , the calculation of running time is conducted based on a microscopically accurate vehicle dynamics model. Figure 2 contains an example of constructing train paths for a train service r , depicting the scheduled route from Station S_1 via S_2 to S_3 . In Figure 2 (a), the utilized block sections are illustrated for the color-highlighted speed-profiles. For example, the speed-profile v_1 possesses $(b_{10}, b_{11}, b_{13}, b_{15}, b_{16}, b_{18}, b_{21})$ as the utilized sequence of block sections. As marginal conditions, it is specified that the initial and final velocities are set to zero. Adhering to these marginal conditions and considering the principles of vehicle dynamics, acceleration occurs to reach a predetermined maximum speed, followed by maintaining a constant speed and deceleration to return to zero velocity. When defining the maximum speed, it is crucial to note the feasibility of decelerating to reach zero velocity. This results in a running time, exemplified by a speed-profile v_1 as shown in Figure 2 (b). This running time also includes the scheduled dwell time at the dispatching point where a speed-profile arrives.

For variations concerning the speed-profiles, the following possibilities are considered:

- (V1) Varying the predetermined maximum speed while maintaining an unaltered sequence of block sections.
- (V2) Altering the sequence of block sections while maintaining a predetermined maximum speed.
- (V3) A combination of varying both the sequence of block sections and the maximum speed.

For speed variation (V1), the initial choice might be a nominal speed predetermined by the timetable. To compensate for delays, a speed-profile with a shorter travel time is generated. Conversely, to avoid catching up to a preceding train, a speed-profile with a longer travel time is generated. In Figure 2 (a), the speed-profiles v_2 and v_3 utilize the same infrastructure, yet due to different maximum speeds, they exhibit varying space-time curves and consequently different travel times (Fig. 2 (b)). Regarding route variation (V2), speed-profiles are initially created for the scheduled train path of the train service, ensuring that following the schedule is always possible. For this purpose, the scheduled platforms for halts are considered as dispatching points, between which speed-profiles are then generated. The route variation process is performed microscopically by deviating from the schedule to approach a different platform during a scheduled halt. An example of this is illustrated by the speed-profiles v_1 and v_4 in Figure 2 (a). Additionally, a macroscopic route variation involves deviating from the schedule between two consecutive, scheduled stations S_1 and S_2 by making one or several additional halts. For an additional halt X , it results in a macroscopic travel sequence (S_1, X, S_2) , where a microscopic route variation occurs again between (S_1, X) and (X, S_2) . Macroscopic route variation between two consecutive, scheduled stations S_1 and S_2 only occurs if the distance covered through the additional halts is not greater than the distance between S_1 and S_2 multiplied by a detour factor $\rho = 2.5$. This method generates a set of speed-profiles $\mathcal{V}(r)$ for a train service r .

3.1.2 Train Path Construction from Speed-Profiles

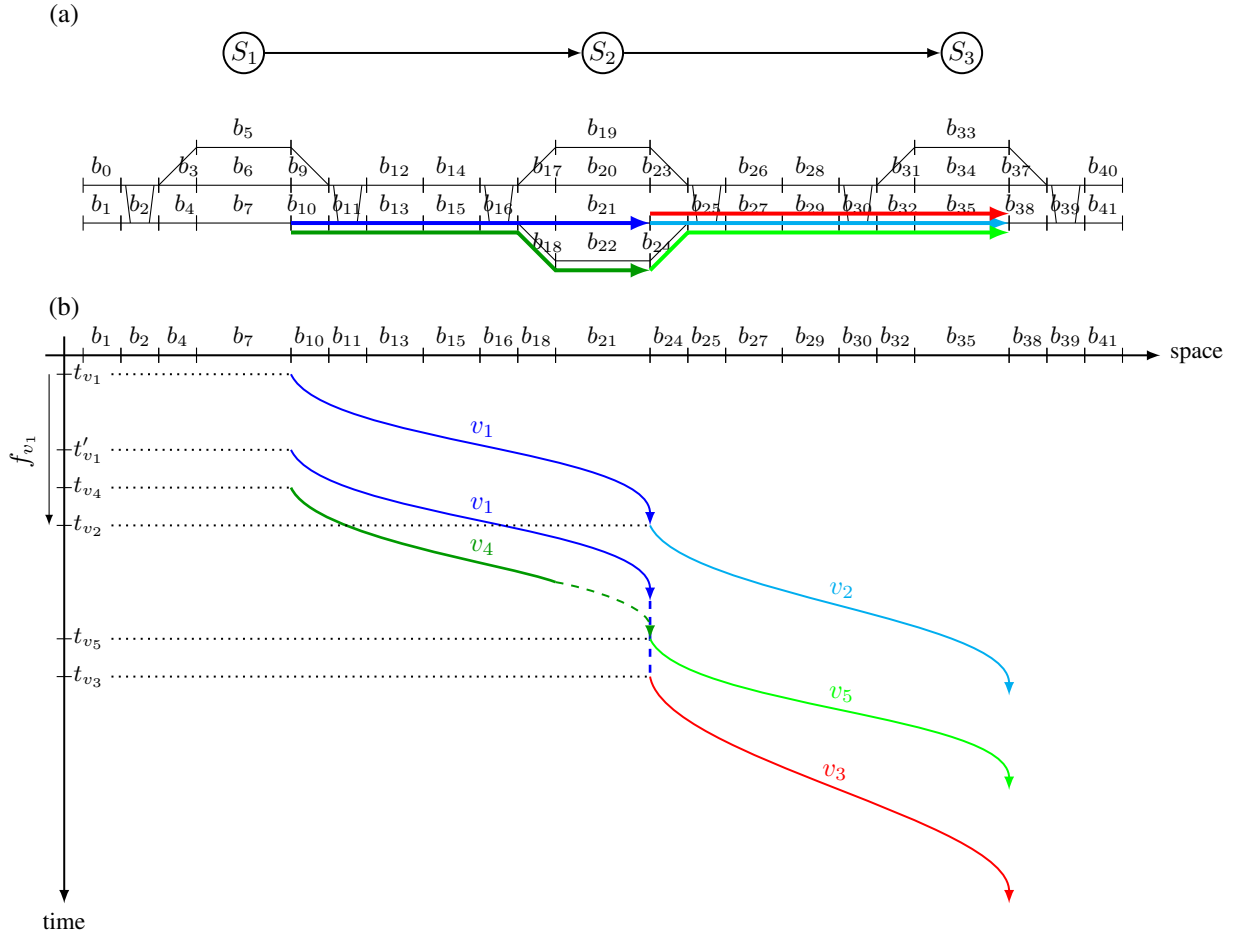


Figure 2: Possible train paths for a train service r from S_1 via S_2 to S_3 . (a) Block sections utilized by the color-highlighted speed-profiles v_1, \dots, v_5 . (b) Space-time curve of the speed-profiles and connection of these to train paths $a_1 = ((v_1, t_{v_1}), (v_2, t_{v_2}))$, $a_2 = ((v_1, t_{v_1}), (v_3, t_{v_3}))$ and $a_3 = ((v_4, t_{v_4}), (v_5, t_{v_5}))$.

Two speed-profiles v, v' can be connected if, from an infrastructural perspective, there is a continuously passable sequence of block sections. Then, for a profile v with $\mathcal{V}(v)$, the set of possible successor speed-profiles is defined. Each v is assigned a departure time t_v , resulting in a pair (v, t_v) . A train path a is then a sequence $((v_i, t_{v_i}))_{i \in \mathbb{N}}$ of these pairs, while adhering to the successor relationships. In Figure 2 (b), three possible train paths are depicted for

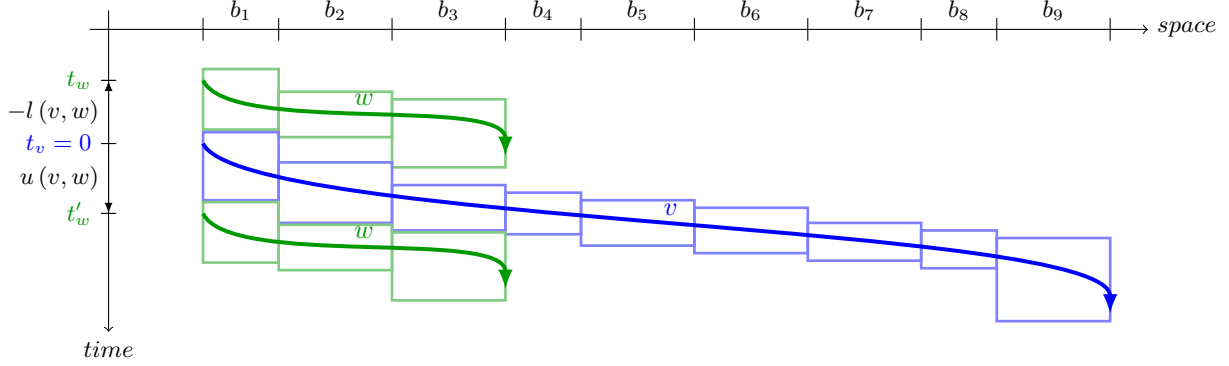


Figure 3: Conflict interval for a speed-profile w defined by a speed-profile v through the minimum headway times $l(v, w)$ and $u(v, w)$.

the illustrated train service. The train paths $a_1 = ((v_1, t_{v_1}), (v_2, t_{v_2}))$ and $a_2 = ((v_1, t'_{v_1}), (v_3, t_{v_3}))$ differ firstly in the choice of the successor speed-profile of v_1 . Additionally, a_2 utilizes a later time point for the departure time of v_1 . Deviating from the other depicted train paths in Figure 2 (b), an additional halt at S_2 is planned for a_2 . With a microscopic rerouting, the train path $a_3 = ((v_4, t_{v_4}), (v_5, t_{v_5}))$ arrives at a different platform.

A train path for a train service r always starts with a start speed-profile and ends with an end speed-profile. The sets for these distinguished speed-profiles are denoted as $\mathcal{V}_{\text{start}}(r)$ and $\mathcal{V}_{\text{end}}(r)$. During the dispatching, start speed-profiles are those speed-profiles that can be chosen when entering the dispatching area. Similarly, end speed-profiles are those chosen when leaving the dispatching area.

3.1.3 Conflict Detection

For two train paths a_1 and a_2 with their parts (v, t_v) and (w, t_w) respectively, there is a potential conflict if v and w share a common block section. (v, t_v) and (w, t_w) are conflict-free if and only if

$$t_w > t_v + u(v, w) \text{ or } t_w < t_v - l(v, w) \quad (1)$$

holds. Here, $u(v, w)$ is the minimum headway time between v and w when w follows v , and $l(v, w)$ is the minimum headway time between v and w when w precedes v . With $-l(v, w)$ and $u(v, w)$, a conflict interval $K(v, w) = [-l(v, w), u(v, w)]$ is defined, and it follows:

$$t_w - t_v \in K(v, w) \iff \text{conflict between } v \text{ and } w \quad (2)$$

In Figure 3, a conflict between two speed-profiles v and w is avoided by choosing a departure time t_w for w such that w departs before v . However, with the choice of t'_w , w could also depart conflict-free after v . Obviously, in this example, $t_w, t'_w \notin K(v, w)$.

In order to avoid conflicts of overtaking or crossing train paths with halting train paths using the same infrastructure, the halting time must be taken into account by enlarging the upper bound of the conflict interval for the planned halting time. This halting time $h(t_w, t_{w'}) = t_{w'} - t_w - f_w$ depends on the succeeding speed-profile w' and its point of time $t_{w'}$. A train path a_1 containing (v, t_v) and a train path a_2 containing the part $(w, t_w), (w', t_{w'})$ will have a conflict, if and only if

$$t_v - t_w \in [-l(w, v), u(w, v) + h(t_w, t_{w'})] \quad (3)$$

or

$$t_v - t_{w'} \in K(w', v). \quad (4)$$

For (3), it follows:

$$\begin{aligned} t_v - t_w &\in [-l(w, v), u(w, v) + h(t_w, t_{w'})] \\ \iff t_v - t_w &\geq -l(w, v) \text{ and } t_v - t_w \leq u(w, v) - f_w \end{aligned} \quad (5)$$

In Figure 4 (a), an example of a halting conflict with a crossing speed-profile v is illustrated. In this case, v traverses block b_3 , which is occupied by the halting of the train path shown in green. Thus, condition (3) is satisfied. Condition (4) is not fulfilled since there is no conflict with w' . Note, that a halting conflict condition $H(v, w, w')$ is described by one speed-profile v of train path a_1 and two succeeding speed-profiles w, w' of train service a_2 and its time points $t_v, t_w, t_{w'}$.

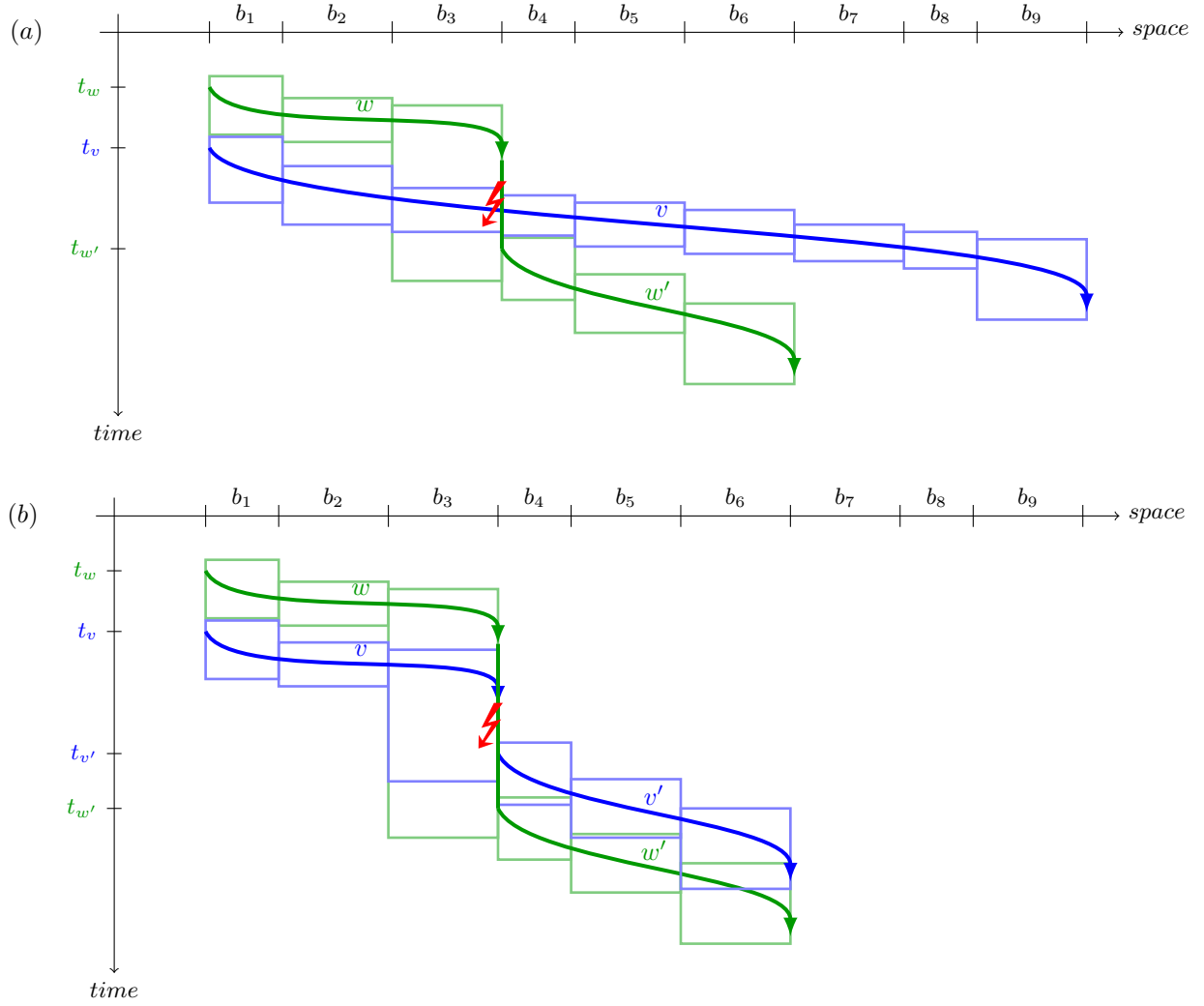


Figure 4: (a) A halting conflict at platform b_3 between a crossing and halting train path with parts (v, t_v) and $(w, t_w), (w', t_{w'})$, respectively. (b) A halting conflict at platform b_3 between two halting train paths with parts $(v, t_v), (v', t_{v'})$ and $(w, t_w), (w', t_{w'})$, respectively.

A halting conflict can also occur between two halting train paths. Let a_1 and a_2 be train paths with parts $(v, t_v), (v', t_{v'})$ and $(w, t_w), (w', t_{w'})$, respectively. In this case, it is sufficient to consider only the halting time $h(t_w, t_{w'})$. However, the departure time $t_{v'}$ must be taken into account, and condition (4) has to be modified. Then, there is a halting conflict between two halting trains if and only if (3) and

$$t_{v'} - t_{w'} \in K(w', v') \quad (6)$$

holds. The example in Figure 4 (b) illustrates a conflict situation in the case of two halting train paths. In this case, conditions (3) and (6) are satisfied, resulting in the detection of a conflict. The halting conflict condition $H(v, v', w, w')$ for two halting train paths is described by two succeeding speed-profiles v, v' of train path a_1 and two succeeding speed-profiles w, w' of train service a_2 and its time points $t_v, t_{v'}, t_w, t_{w'}$.

3.2 PMC-CG

3.2.1 Path-oriented IP Formulation

In the path-based formulation, a path represents a sequence of speed-profiles, in other words, a train path. For each train path, a binary variable is introduced as follows:

$$x_a = \begin{cases} 1 & , \text{ if train path } a \text{ is selcted} \\ 0 & , \text{ otherwise} \end{cases}$$

Moreover, c_a denotes the cost associated with train path a . In this context, the costs represent the delay incurred by train path a when leaving the dispatching area. The TDP now involves selecting a train path from the set of all possible train paths for each of the train services. Here, the train services considered are those located within the dispatching area and time horizon. This selection of train paths must be conflict-free. In this paper we will use column generation for solving the relaxation. When using column generation for a mixed integer problem, the pricing steps are usually performed within the relaxation. Hence, it is very important to have a very strong model formulation. Instead of using pairwise conflict constraints, it is much more stronger to use maximum conflict cliques. A clique naturally arises, if a subset of train paths uses one common block of infrastructure. Those block based cliques are not necessarily maximum. Here, a cross-block conflict consideration takes place. Block-crossing means that cliques are formed by considering conflicts not only within a single block section but across block sections related to the entire train path. Thus, this approach examines network-wide interconnections of conflicts. Train path-based cliques correspond in form to the path-based cliques described in [Caprara \(2010\)](#), which, as described there, generally represent a stronger LP formulation. The modelling of conflicts is thus carried out using train path-based maximal cliques C within an undirected conflict graph $G = (\mathcal{A}, \mathcal{E})$. In this graph G , the set of nodes is represented by the train paths $a \in \mathcal{A}$, and there is an edge $(a_1, a_2) \in \mathcal{E}$ if there is a conflict between a_1 and a_2 . The entire conflict situation is described by \mathcal{C} , the set of all maximal cliques C . In the IP, these cliques are formulated in the form of set-packing constraints. With the objective of the TDP, the following complete model is then derived:

$$\sum_{a:a \in \mathcal{A}} c_a x_a \rightarrow \min \quad (7)$$

$$\forall r \in \mathcal{R} : \sum_{a:a \in \mathcal{A}(r)} x_a = 1 \quad (8)$$

$$\forall C \in \mathcal{C} : \sum_{a:a \in C} x_a \leq 1 \quad (9)$$

$$x_a \in \{0, 1\}, a \in \mathcal{A} \quad (10)$$

The objective function (7) minimizes the costs of the train paths. Constraint (8) ensures that exactly one train path is selected for each train service $r \in \mathcal{R}$. This condition is known as the fulfillment condition. With (9), it is ensured, that at most one train path is selected from every C , ensuring conflict-free selections. Constraint (10) represents the integrality condition for the variables x_a . The set \mathcal{A} contains all possible train paths for all train services $r \in \mathcal{R}$. The number of train paths in \mathcal{A} is very high because for every possible sequence of speed-profiles, there can be a different choice of departure times.

3.2.2 Flow of the PMC-CG

The PMC-CG uses column generation to solve (7) - (10). Column generation searches for new columns for the LP relaxation of the restricted master problem (rRMP), which means to minimise

$$z(rRMP) = \min \left\{ \sum c_a x_a \mid (7) - (9), x_a \geq 0, a \in \mathcal{A}' (\subseteq \mathcal{A}) \right\}. \quad (11)$$

Note, that the total optimum of TDP is

$$z(TDP) = \min \left\{ \sum c_a x_a \mid (7) - (9), x_a \in \{0, 1\}, a \in \mathcal{A} \right\}. \quad (12)$$

If there are train paths a_{new} with negative reduced costs $\rho_{a_{new}}$, the variable $x_{a_{new}}$ associated with a_{new} is added to the rRMP as a new column, expanding the set \mathcal{A}' with a_{new} . The determination of $\rho_{a_{new}}$ is based on the dual variables α_r and β_C related to the fulfillment conditions (8) and clique inequalities (9), respectively. The reduced costs are computed as follows:

$$\forall r \in \mathcal{R} : \rho_{a_{new}} = c_{a_{new}} + \sum_{C \in \mathcal{C}: a_{new} \in C} \beta_C - \alpha_r \quad (13)$$

Here, $c_{a_{new}}$ represents the costs of the new train paths, indicating their delay upon leaving the dispatching area. Since α_r remains constant, the subproblem for each train service $r \in \mathcal{R}$ becomes:

$$\rho^*(r) = \min \left\{ c_{a_{new}} + \sum_{C \in \mathcal{C}: a_{new} \in C} \beta_C \mid a_{new} \text{ is a train path for train service } r \right\} \quad (14)$$

The flow of the PMC-CG is depicted in Figure 5. The feasible initial solution with the subset $A' \subseteq A$ for column generation is determined using a first-come-first-serve (FCFS) start heuristic. Here, the train services are sorted based on their arrival time in the dispatching area. Successively, for each train service, a conflict-free train path is generated added to rRMP².

In order to keep the algorithm online, the method terminates, if either a good solution quality or a time limit has been reached. The quality of the solution is evaluated by the optimality gap, which can be calculated from a lower bound. Following Desrosiers and Lübbecke (2005) and Lübbecke (2011), Lagrangian relaxation of the conflict constraints (9) provides a good lower bound:

$$lb(rRMP) = z(rRMP) - \sum_{r \in \mathcal{R}} \rho^*(r) \leq z(TDP), \quad (15)$$

where $z(rRMP)$ is the actual objective value of the rRMP. Since our method solves the subproblems by optimality, we are able to compute those values.

While adding new train path variables to the rRMP the system of clique constraints must be updated. Some conflict cliques have to be enlarged and new maximum conflict cliques (= new rows) will arise. This is an essential part of the PMC-CG and is described in Section 3.2.4. After finishing the column generation process, a possibly non-integer solution causes to calculate the final integer solution of the restricted master problem (RMP).

3.2.3 MIP Subproblem

Upon examining (14), it is evident that solving this minimisation problem involves deciding whether a_{new} belongs to a maximal clique C or not. This occurs when a_{new} conflicts with all $a \in C$. The pricing with β_C can be avoided by avoiding the conflict with at least one $a \in C$. This can be achieved through rerouting, that is selecting a different sequence of profiles. Alternatively, it could involve rescheduling by adjusting the departure times of speed-profiles or simultaneous rerouting and rescheduling. Typically, these actions result in higher costs $c_{a_{new}}$ due to longer travel times on detours or additional unplanned halts and dwell times. The network-wide conflict consideration in the individual $C \in \mathcal{C}$ now makes it challenging to determine where and how rerouting and rescheduling should occur to achieve the best possible trade-off between costs $c_{a_{new}}$ and β_C , leading to minimal reduced costs.

This decision is made through a MIP. Let t_e denote the time of the train path a_{new} after using an end speed-profile. For all $v \in \mathcal{V}_{end}(r)$, $t_e = t_v + f_v$ holds. The end speed-profile ends at a dispatching point, defining the location where the dispatching area is left. Then, t_e is the point of time when the dispatching area is left. The cost $c_{a_{new}}$ results from the difference between t_e and the scheduled time $t_e^{scheduled}$ at this designated dispatching point according to the timetable. A feasible train path is obtained by considering the successor conditions of speed-profiles, which can be realized through flow conservation (Eq. (16) and (17)), precedence constraints (Eq. (18) - (20)), and the binary variables:

$$y_v = \begin{cases} 1 & , \text{ if speed-profile } v \text{ is selcted} \\ 0 & , \text{ otherwise} \end{cases}$$

The following constraints arise as a result:

$$\sum_{v: v \in \mathcal{V}_{start}(r)} y_v = 1 \quad (16)$$

$$\forall v \in \mathcal{V}(r) : y_v - \sum_{v': v' \in \mathcal{V}_{suc}(v)} y_{v'} = 0 \quad (17)$$

$$\forall v \in \mathcal{V}_{start}(r) : t_v \geq t_b \quad (18)$$

$$\forall v \in \mathcal{V}(r), v' \in \mathcal{V}_{suc}(v) : t_{v'} \geq t_v + f_v y_v \quad (19)$$

$$\forall v \in \mathcal{V}_{end}(r) : t_e = t_v + f_v y_v \quad (20)$$

²This is done by solving the subproblem. When a new train path is generated for a train service, new conflict cliques C can arise. If there are conflict cliques, they will be included in the subproblem and the corresponding β_C will be set to ∞ . Then, the subproblem will be solved again. This is carried out, as long as new conflict cliques are detected. If not, there is a conflict free train path for the current train service and it continues with the next train service. This ensures a consistent avoidance of conflicts described by C , whereby rerouting and rescheduling also take place.

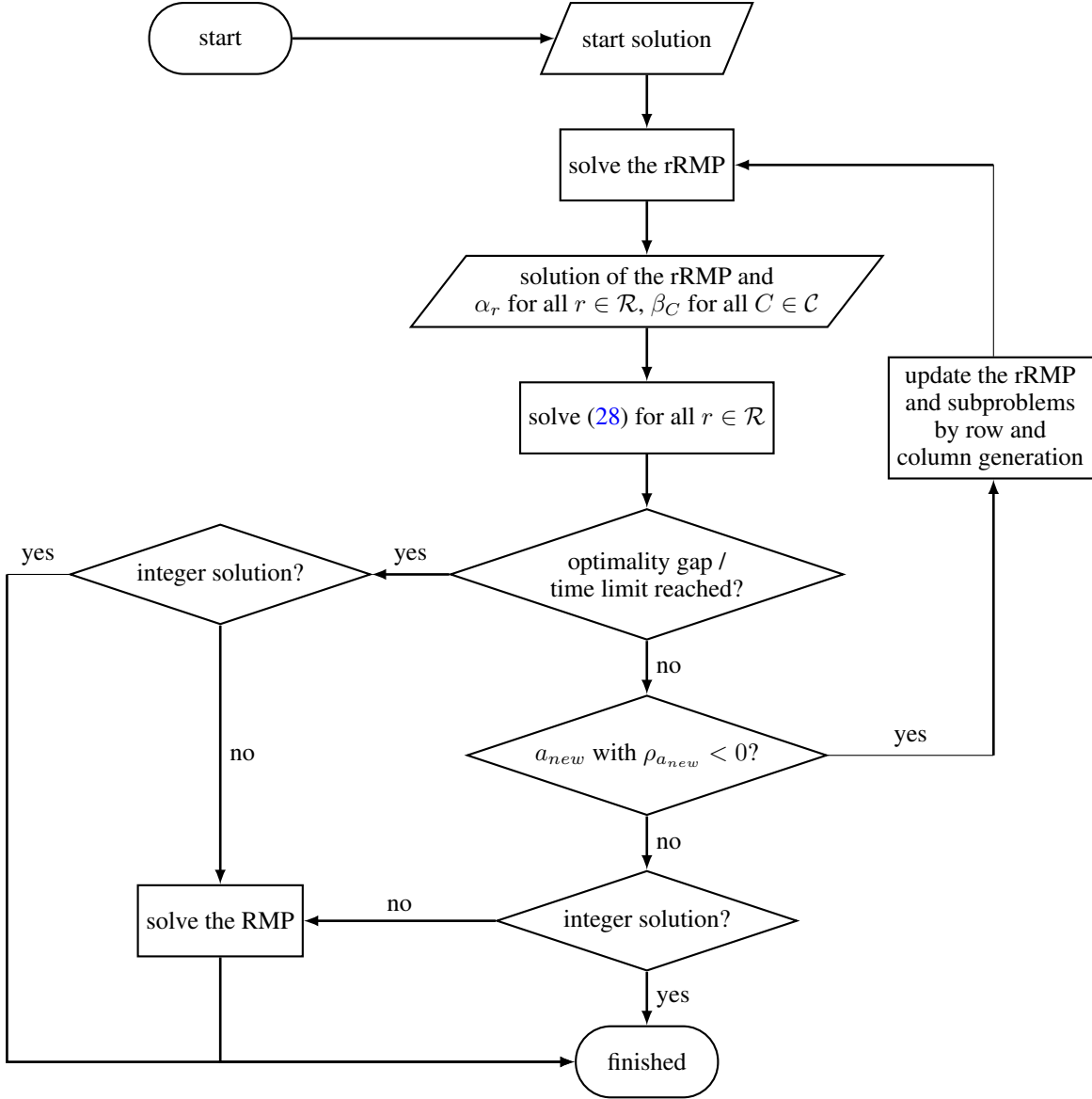


Figure 5: Overview of the PMC-CG

A train path can only start with a starting speed-profile, as ensured by (16). With (17), exactly one successor must be selected for a speed-profile v . Specifically, for the starting speed-profiles, (18) ensures that their departure cannot be before t_b , that is the entry time into the dispatching area. If a speed-profile v is chosen, then according to (19), for a successor speed-profile w , the departure time of w must be greater equal than the departure time of v plus its running time f_v . It should be noted that in the case where $t_{v'} > t_v + f_v y_v$ with $y_v = 1$, there is an extended halt beyond the minimum dwell time before the departure of v' . Condition (20) provides the point of time when leaving the dispatching area.

The decision whether a_{new} belongs to a maximal clique C initially involves checking for a conflict with a train path. This process is carried out for all $a \in \bigcup_{C \in \mathcal{C}} C \subseteq \mathcal{A}'$. Following condition (2) the conflict detection can be made with means of the conflict intervals and binary indicator variables z_K^l, z_K^u . This results in the following conditions.

$$\forall K(w, v) \in \mathcal{K} : t_v \leq t_w - l(w, v) + M(z_K^l - y_v + 1) - \varepsilon \quad (21)$$

$$t_v \geq t_w + u(w, v) - M(z_K^u - y_v + 1) + \varepsilon \quad (22)$$

Here, \mathcal{K} is the set of all conflict intervals $K(v', v)$ that must be considered for the speed-profiles $v \in \mathcal{V}(r)$ of the train service r . The speed-profiles w are those that are already used by generated train paths $a \in \mathcal{A}'$. The $\varepsilon > 0$ values are

sufficiently small so that (21) and (22) indeed represent strict less-than and strict greater-than conditions, and $M > 0$ values are sufficiently large. Constraints (21) and (22) are active only when the respective speed-profile v is chosen, i.e., $y_v = 1$. With $y_v = 1$, in case of a conflict, i.e., (2) holds, this implies $z_K^l = z_K^u = 1$. With a binary variable z_a and

$$\forall a \in \mathcal{A}' : Mz_a \geq \sum_{K:K \in \mathcal{K}(a)} (z_K^l + z_K^u - 1) \quad (23)$$

a conflict with a train path a can be detected. $\mathcal{K}(a) \subseteq \mathcal{K}$ is the set of conflict intervals that must be considered for the conflict detection between the train path a with the new train path to be generated for r . If at least one conflict interval $K(v', v) \in \mathcal{K}(a)$ exists such that $t_v \in K(v', v)$, then $z_a = 1$, indicating the conflict with a .

If conditions (3), (4) and (6) hold, a halting conflict arises. Since condition (4) and (6) are already included in (21) - (23) we must only consider (3). With (5) it follows:

$$\forall H(v, w, w') \in \mathcal{H} : t_v \leq t_w - l(w, v) - M(z_H^l - y_v + 1) + \varepsilon \quad (24)$$

$$t_v \geq t_{w'} + u(w, v) - f_w + M(z_H^u - y_v + 1) - \varepsilon \quad (25)$$

$$\forall a \in \mathcal{A}' : Mz_a \geq \sum_{H:H \in \mathcal{H}(a)} (z_H^l + z_H^u - 1) \quad (26)$$

Here, we also use binary indicator variables z_H^l, z_H^u to decide if $t_v - t_w \in [-l(w, v), u(w, v) + h(t_w, t_{w'})]$. This is carried out for every $v \in \mathcal{V}(r)$, where all corresponding $H(v, w, w')$ will be considered. \mathcal{H} is set of all halting conflict conditions³. In (24) and (25), appropriately small ε and large M values must be chosen. If the speed-profile v is not chosen, the constraints (24) and (25) become inactive. Otherwise a halting conflict is detected if $z_H^l = z_H^u = 1$ and with (26) then $z_a = 1$ and thus a conflict with a follows. For this purpose, constraint (26) uses the set $\mathcal{H}(a) \subseteq \mathcal{H}$, which is the set of halting conflict conditions that must be considered for the potential halting conflicts with a . With variables z_a and the constraint

$$\forall C \in \mathcal{C} : z_C \geq \left(\sum_{a:a \in C \in \mathcal{C}} z_a \right) - |C| + 1, \quad (27)$$

the binary variable z_C determines whether a_{new} belongs to a maximal clique C . Here, $|C|$ represents the cardinality of C . The right-hand side of (27) becomes one if conflicts exist with all $a \in C$, consequently resulting in $z_C = 1$. Using $z_C \beta_C$ for all $C \in \mathcal{C}$, the MIP subproblem models the costs for conflicts in the objective function. The resulting complete MIP subproblem for each $r \in \mathcal{R}$ is formulated as follows:

$$(t_e - t_e^{scheduled}) + \sum_{C:C \in \mathcal{C}} z_C \beta_C \rightarrow \min$$

$$s.t. \quad (16) - (27) \quad (28)$$

$$t_v, t_w, t_e \geq 0, y_v, y_w, z_K^l, z_K^u, z_H^l, z_H^u, z_a, z_C \in \{0, 1\}$$

3.2.4 Determining and Updating the Maximal Cliques

An essential component of the PMC-CG presented here is the determination and updating of the maximal cliques. When new train paths are generated by solving the subproblems (28) for all $r \in \mathcal{R}$, the clique inequalities (9) must be supplemented with the respective variables or new inequalities created. Let a_{new} be a newly generated train path for a train service r . The conflict graph $G = (\mathcal{A}', \mathcal{E})$ is then expanded by this train path, i.e., $\mathcal{A}' \leftarrow \mathcal{A}' \cup \{a_{new}\}$. Through conflict detection (Sect. 3.1.3), conflicts between a_{new} and $a \in \mathcal{A}' \setminus \{a_{new}\}$ are identified, and corresponding edges (a_{new}, a) in G are generated and added to the set of edges. In G extended by a_{new} , maximal cliques C' are now sought. Since only the maximal cliques involving a_{new} are of interest, the search is performed in the subgraph of G induced by a_{new} denoted as $G(a_{new}) = (\mathcal{A}_{a_{new}}, \mathcal{E}_{a_{new}})$. The set of nodes $\mathcal{A}_{a_{new}}$ consists of a_{new} and every $a \in \mathcal{A}'$ having a conflict with a . For two nodes $a_1, a_2 \in \mathcal{A}_{a_{new}}$ there exists an edge (a_1, a_2) if a_1, a_2 have a conflict. The detection of the set of the maximal cliques \mathcal{C}' in $G(a_{new})$ is carried out using the algorithm by Tomita (2017), an extension of the algorithm by Bron and Kerbosch (1973). Among these cliques $C' \in \mathcal{C}'$ containing a_{new} , a comparison is made to decide which clique $C \in \mathcal{C}$ needs to be expanded by a_{new} . For every C' , a subclique $C = C' \setminus \{a_{new}\}$ is searched, which is then extended by a_{new} , and the variable $x_{a_{new}}$ is added to the corresponding clique inequality (9) in the rRMP. If there is no such sub-clique C for C' meeting the described conditions, then C' is a new maximal clique, and thus $\mathcal{C} \leftarrow \mathcal{C} \cup \{C'\}$ follows along with the generation of a new clique inequality for C' in the rRMP, that is a row generation process.

³It's easy to see that a similar condition holds for the case of two halting trains $H(v, v', w, w')$ (Sect. 3.1.3).

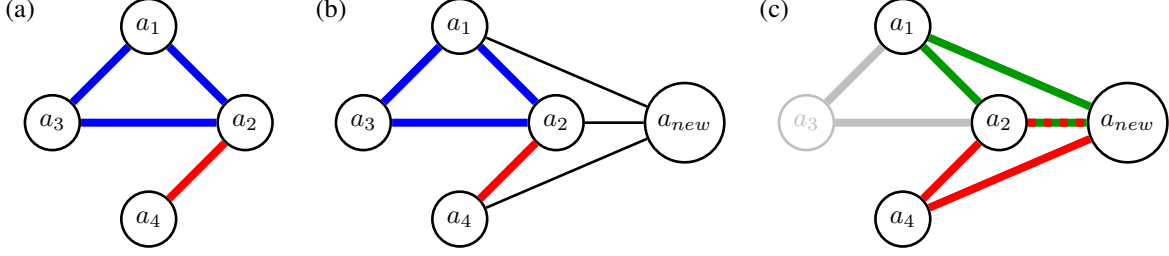


Figure 6: Schematic representation of updating existing and detecting new maximal cliques. (a) Conflict graph without the new train path a_{new} . (b) Conflict graph with the new train path a_{new} . (c) Highlighted subgraph induced by a_{new} with the updated (marked in red) and new (marked in green) maximal cliques.

The process for updating the maximal cliques is depicted in Figure 6. In Figure 6 (a), the conflict graph G shows the existing maximal cliques $C_1 = \{a_1, a_2, a_3\}$ and $C_2 = \{a_2, a_4\}$. A train path a_{new} conflicts with the train paths a_1 , a_2 , and a_4 resulting in the extended conflict graph (Fig. 6 (b)). In the subgraph of G induced by a_{new} , the maximal cliques $C'_1 = \{a_1, a_2, a_{new}\}$ and $C'_2 = \{a_2, a_4, a_{new}\}$ exist (Fig. 6 (c)). For C_2 , only C'_2 satisfies $|C_2| = |C'_2| - 1$, indicating that C_2 is a potentially updated clique. Moreover, since $|C_2| = |C'_2| \setminus \{a_{new}\}$ holds, C_2 will be updated. For C'_1 , neither C_1 nor C_2 meets these conditions, resulting in the addition of C'_1 as a new clique.

With the new train path a_{new} , the updated and newly generated maximal cliques, the individual subproblems for the train services are also updated. For the new train path, the constraints (21) - (26) are generated in the subproblem (28) of every $r \in \mathcal{R}$. For each subproblem, for an updated clique C , the associated constraint (27) is supplemented with the variable $z_{a_{new}}$, and for a newly generated maximal clique, such a constraint is added to the subproblem (row generation).

4 Numerical Experiments

4.1 Scenario Description

The dispatching area considered for the evaluation of the algorithm is located in the northern part of Bavaria, around Nuremberg (NN) (Fig. 7). Deutsche Bahn provides infrastructure data on the railway lines (DB). The Bavarian scenario was extracted from this database. The database includes informations on speed limits, block sections, junctions, single and double track lines (Fig. 8 (a),(b)). From this, speed-profiles with minimum headway times can be constructed on the tracks. Due to the lack of information on the infrastructure within railway stations, we use a simplified transit matrix. Arrival and departure nodes are connected via edges (Fig. 8 (c)). For speed-profiles with geometrically crossing transit edges a minimum headway is generated within the preprocess. Halting positions on the transit edges were inserted to the best of our knowledge.

Speed-profiles were constructed for regional and long distance trains for this scenario. Stopping patterns of the train services had been taken from a real-world timetable. Entry and exit nodes of the dispatching area as well as halting points were defined as dispatching points, the speed-profiles were generated according to Section 3.1.1. Dispositive stops on open tracks are not considered in our scenario. From a railway operations perspective, this leads to wasted capacity since trains are held at stations to give priority to other trains. Otherwise, trains could leave the station and let other trains pass at intersections, thereby not unnecessarily blocking platforms for extended periods. The focus of this work is on the methodological approach and its performance rather than on an exact optimisation of the real-world capacity.

In the dispatching area, we consider $n \in \{40, 50, 60\}$ train services, including both long-distance and regional trains. For these train services with their scheduled stops, macroscopic travel paths are generated. Based on this, the speed-profiles are generated as described in Section 3.1.2.

In order to analyse the performance of the PMC-CG with respect to different routing options, the full set $\mathcal{V}(r)$ generated according to Section 3.1.1 is reduced by considering only the speed-profiles of at most k shortest paths from entry to the exit points of the train service r . We call k the reduction index. $k = \infty$ means, that we may use the full but finite set of speed-profiles. The path of the individual train services cut the dispatching area in different sizes, so that there are not always k paths available.

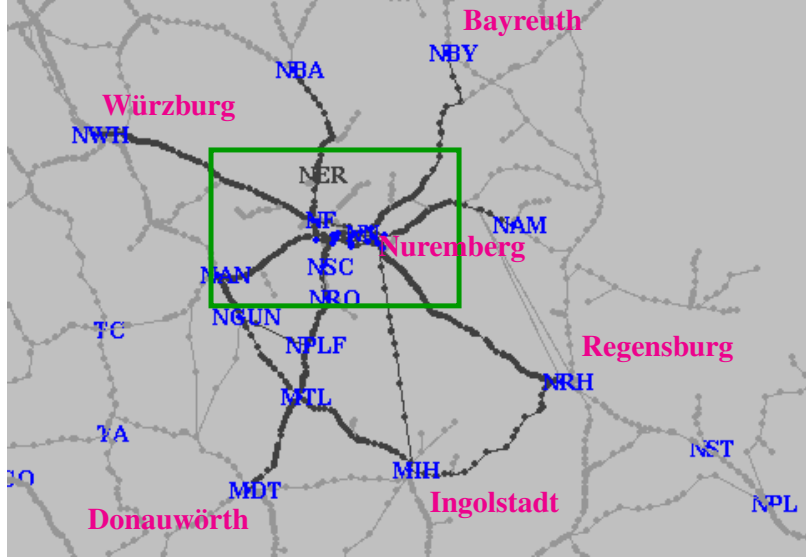


Figure 7: Dispatching area in the region of northern Bavaria around Nuremberg.

Table 1 displays the number of spacial routing options for the different instances⁴.

Table 1: Total routing options for different number n of train services when limiting the maximum routing options to k .

$n \backslash k$	100	300	500	750	∞
40	1148	2346	3056	4602	5916
50	1279	2479	3679	5177	6443
60	1367	2567	3767	5267	6533

For the scenarios we consider train services with a regular, conflict-free timetable within a time horizon of approximately one hour. The arrival times for these train services are subject to a disturbance d which was modelled by the following probability function (Schwanhäußer, 1974):

$$P(D \leq d) = \begin{cases} 0 & , \text{ if } d < 0 \\ 1 - (1 - q) e^{-\lambda d} & , \text{ if } d \geq 0 \end{cases} \quad (29)$$

Positive delays follow an exponential distribution with the parameter λ and $1 - q$ represents the proportion of disturbed train services. This approach gives us a railway operation situation for the TDP. Disruption scenarios can range from (minor) disturbances to longer interruptions. From the boxplots in Figure 9 (sample size = 700), it can be seen that, for the scenarios, delays in the range of minor disturbances are considered. Due to the chosen distribution (29) of the initial delays, the average is approximately 300 seconds in both cases. From the boxplots in the upper left and lower left in Figure 9, it can be observed that 50% of the values fall within the range of 100 to 400. For the scenarios, there are outliers above 1000 seconds.

In the Following, a scenario is encoded as NN- n - k . Here, NN designates the aforementioned dispatching area. For each scenario, 50 computations were performed with disturbances following Equation (29) and fixed parameters $q = 0.8$ and $\lambda = \frac{1}{300} \frac{1}{s}$. All tests were conducted on an Intel Core i7-8550U CPU @ 1.80GHz with 16 GB RAM. The PMC-CG is implemented in C++, and the IP, LP and MIP models are solved using the Gurobi solver (v9.0.1).

⁴The actual number of available routing options within the reduced set of speed-profiles may be larger than the number of k shortest path.

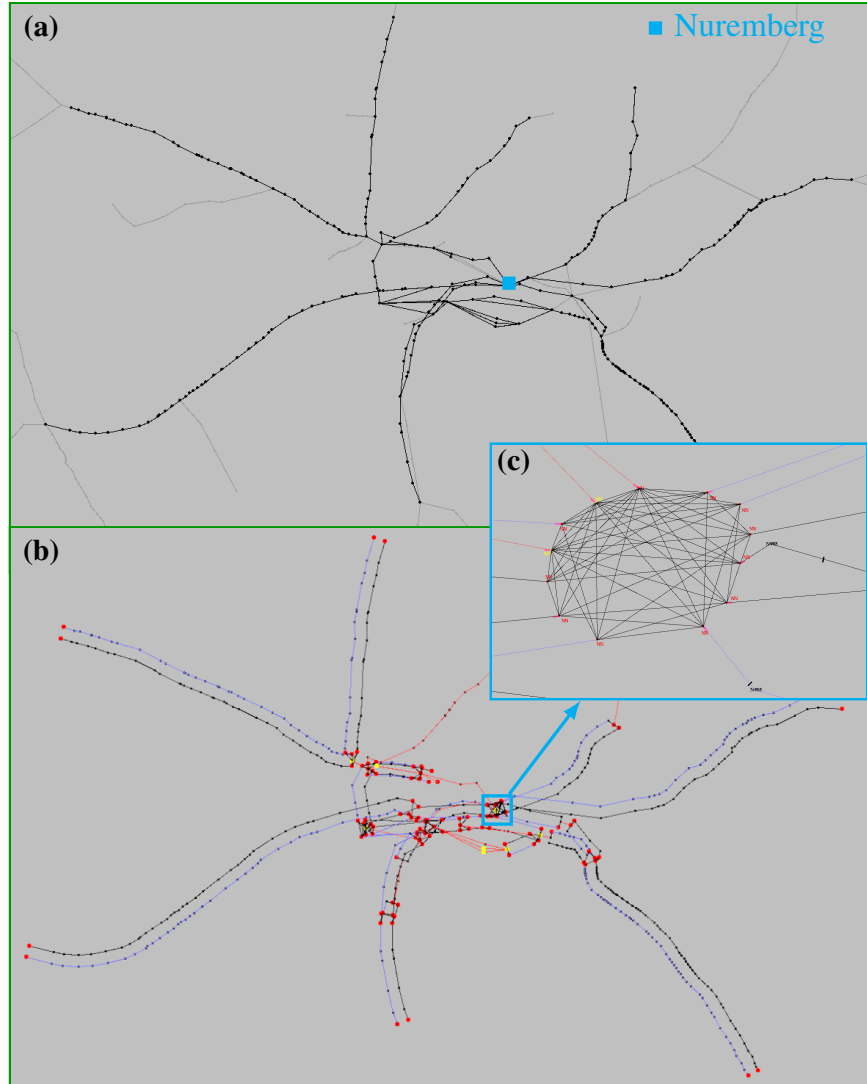


Figure 8: (a) A section of the operating point graph for the vicinity of Nuremberg Central Station (see Figure 7). (b) The infrastructure with block sections, single-track (red), and double-track (black and blue) lines based on the operating point graph in (a). (c) Connections for traversing Nuremberg Central Station.

4.2 Results

4.2.1 Complexity and Runtime Behaviour PMC-CG

In a first experiments we apply the PMC-CG without any time limit in order to get the optimal solution. The number of train services in the dispatching area and the reduction index k will be varied. We consider the scenarios NN- n - k with $n \in \{40, 50, 60\}$ and $k \in \{100, 300, 500, 750, \infty\}$. Table 2 contains the average number of generated train paths. More train services in the scenarios lead to more train paths (variables x_a) being generated, whereas the reduction index does not have such a strong influence.

In Table 3, the conflict situation for the individual scenarios is presented. As expected, this situation becomes more complex with a higher number of train services. The average number of cliques increases much more when the number of trains is increased, compared to an increase in routing options.

For the scenarios NN- n - k with $n \in \{40, 50, 60\}$ and $k \in \{100, 300, 500, 750, \infty\}$, Table 4 shows the average, minimum and maximum computation time. It turns out that with a number of train services of 40, the average computation times are almost constant across different maximum routing options. Regarding the maximum computation time, it can be seen from Table 4 that there is an impact of the routing options for $n = 50$ and $n = 60$.

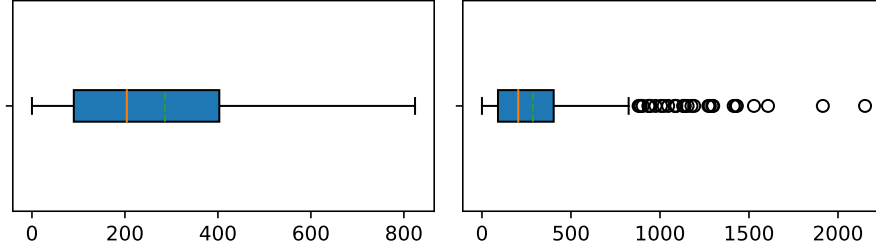


Figure 9: Boxplots of the initial disturbances for the scenarios.

Table 2: Average number of generated train paths (variables x_a) for scenarios with different n and k .

$n \backslash k$	100	300	500	750	∞
40	63.86	59.18	60.98	62.2	58.82
50	98.96	112.30	115.44	105.8	118.36
60	151.98	156.44	146.42	145.48	156.86

Table 3: Conflict situation (average number of cliques / average clique size) for different maximum routing options and number of train services.

$n \backslash k$	100	300	500	750	∞
40	41.86 / 3.63	31.78 / 3.31	36.88 / 3.51	39.06 / 3.80	42.22 / 3.43
50	100.46 / 4.45	141.30 / 5.14	150.70 / 5.67	189.46 / 5.31	207.52 / 5.87
60	316.58 / 5.83	250.36 / 6.67	236.94 / 5.99	480.64 / 6.39	475.26 / 6.34

As can be seen from Table 1, scenarios with 50 and 60 train services have almost identical total routing options. However, the computation times differ significantly (Tab. 4). Hence, the number of train services has a greater influence on the runtime behavior.

The higher computation times are associated with the conflict situation (cf. Tab. 3 and 4). The increased computation times with more existing cliques result from the process of updating cliques. Here, a search for maximal cliques takes place, which is known to be a challenging problem. This can also explain the computation time for $n = 60$ and $k = 100$, as there were configurations that led to an „unfavorable“ conflict situation. Here too, limiting the computation time is of crucial importance for real-world applications.

Table 4: Computation times (average / minimum / maximum) [s] for different maximum routing options and number of train services.

$n \backslash k$	100	300	500	750	∞
40	2.6 / 0 / 14	2.06 / 0 / 10	2.32 / 0 / 14	2.63 / 1 / 20	3.86 / 1 / 105
50	11.8 / 1 / 88	15.65 / 2 / 147	17.54 / 0 / 158	16.56 / 1 / 198	41.08 / 4 / 1187
60	63.66 / 2 / 1237	47.38 / 1 / 376	47.6 / 1 / 550	84.16 / 0 / 1316	96.62 / 3 / 1210

For the scenario NN-60- ∞ and the case with the maximum computation time of 1210 seconds, the computation times for each iteration of column generation are shown in Figure 10. The computation times grow exponentially. Hence, for real-world applications, it is advisable to terminate the column generation prematurely. The optimality of the solution is then not proven, but a high-quality solution may be obtained. To investigate this, the quality of the PMC-CG will be evaluated in the following section.

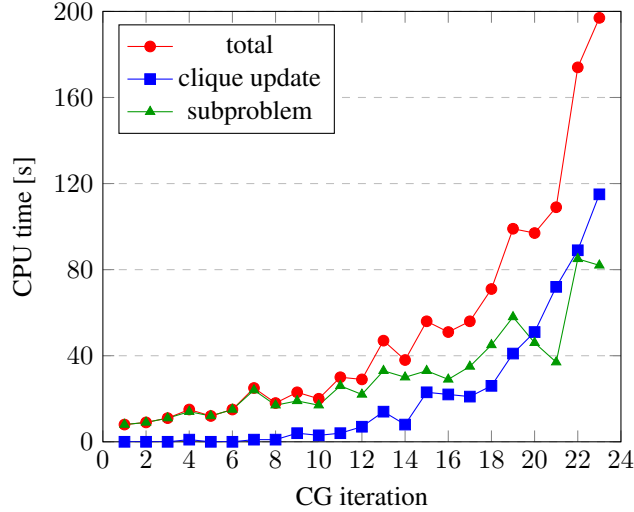


Figure 10: Computation time (CPU time) for the column generation iterations.

4.2.2 Quality of the PMC-CG under Real-Time Requirements

Further numerical computations aim to evaluate the quality of the algorithm under real-time conditions. For this purpose, two scenarios NN-60- ∞ are chosen, where the maximum computation time for the online capability of the algorithm is set to 60 seconds. In the first scenario, a minimum optimality gap (following only referred to as gap) of 0 is chosen, and in the second scenario, the gap is set to 0.1. Column generation suffers from the tailing-off effect (Desrosiers and Lübbecke, 2005), so it is intended to terminate prematurely at a gap of 0.1. To assess the quality, the results of both scenarios will be compared with the scenario NN-60- ∞ with no restriction on the computation time and gap. The quality of the algorithm will be measured based on the delay quotient $\frac{d_{start}}{d_{end}}$. Here, d_{start} is the total delay of the considered n train services after the FCFS start heuristic, and d_{end} is the delay after the termination of the column generation.

Table 5: Numerical results with and without computation time limits.

NN-60- ∞		delay quotient	CPU time [s]	GAP [%]	integer [%]	#cliques	#iterations
gap = 0,	max CPU time = 60s	47.53	18.7	2.0	92.0	152.9	6.96
gap = 0.1,	max CPU time = 60s	49.80	16.26	20.0	92.0	178.74	5.06
gap = 0,	max CPU time = 60s	47.31	96.62	0.0	98.0	475.26	9.62

Table 5 presents the results for the described scenarios with different restriction to the minimum computation time and gap. Column 1 of Table 5 contains the delay quotient. Column 2 indicates the average computation time (CPU time) of the algorithm (PMC-CG). The optimality gap after the termination of the PMC-CG (GAP) is listed in Column 3, and Column 4 contains the proportion of integer solutions after the termination of PMC-CG. The penultimate column of Table 5 displays the average number of cliques, and the last column lists the average number of iterations of column generation. Despite imposing constraints on the gap and computation time, the delay quotient demonstrates that the delay was reduced nearly equally well in all three scenarios, particularly for the scenarios with a zero gap. These restrictions significantly reduced the computation time, meeting real-time requirements. For the scenario with a gap of 0.1, the average computation time was further reduced by approximately 2.5 seconds, with only a minimal decrease in solution quality. Table 5 further shows, that the PMC-CG provided at least 92% integer solutions. Again, the number of cliques corresponds with the computation time. In the scenario without constraints on the gap and computation time, an average of three to four additional iterations were performed. This indicates that in the final iterations of column generation, a large number of new cliques are generated, making the problem increasingly complex. This also makes it challenging to solve subproblems within an acceptable time (cf. Fig. 10). Early branching is a common method for accelerating column generation (Desaulniers et al., 1999). However, after the pricing a high remaining optimality gap at the root node of the branching tree poses a greater risk that the branch-and-price algorithm may be less effective (Maher and Rönnberg, 2023). Nevertheless, for the scenario with zero gap and a maximum computation time of 60 seconds, the gap is only 2%, mitigating this risk, and a high-quality solution is already present at the root node.

5 Conclusion

In this paper, a column generation approach for solving a path-oriented model for the Train Dispatching problem is presented. A major novelty is the modelling of conflicts as maximum cliques which have to be modified dynamically during column generation. The resulting difficult problem of taking into account the shadow prices of cliques when calculating new train paths was formulated by a MIP and can be solved efficiently and quickly in practical use. The strong formulation using path-based cliques provides good candidates for constructing integer solution after the column generation process. This statement is supported by the observation that the relaxation very often provides integer solutions.

The separation between the calculation of speed profiles and the optimization of entire train paths allows a flexible use of infrastructure and driving dynamics calculations in different granulations and by different program systems.

The generation of speed-profiles based on real-world infrastructure is a topic for further research. With that, the PMC-CG can and needs to be tested on more complex real-world instances. The shown computation times and the quality of the solutions promise good results even when applied to such instances.

Another advantage of column generation results from its use in the context of a rolling horizon approach. With the PMC-CG, the train paths are generated for the entire spatial observation space and can thus break out of the time horizon in time under certain circumstances. If the time horizon is now shifted in discrete time steps for the fixed spatial observation space (rolling horizon approach), the generated train paths retain their validity. Hence, the generated train paths can be used in subsequent optimization runs of the rolling horizon approach, where good lower bounds may already be available at the beginning of column generation, promising an advantage in terms of computation times and solution quality.

Dispatching only takes place within the dispatching area. Possible effects beyond this area are not considered when applying dispatching measures. For the PMC-CG, there is the possibility to formulate effects outside the dispatching area, such as connection or circulation conditions, in the form of cost functions and to integrate them into the objective function of the pricing problem.

References

- A. Bettinelli, A. Santini, and D. Vigo. A real-time conflict solution algorithm for the train rescheduling problem. *Transportation Research Part B: Methodological*, 106:237–265, 2017. ISSN 01912615. doi:[10.1016/j.trb.2017.10.005](https://doi.org/10.1016/j.trb.2017.10.005).
- P. Bonami, A. Lodi, A. Tramontani, and S. Wiese. On mathematical programming with indicator constraints. *Mathematical Programming*, 151(1):191–223, 2015. ISSN 14364646. doi:[10.1007/s10107-015-0891-4](https://doi.org/10.1007/s10107-015-0891-4).
- R. Borndörfer and T. Schlechte. Models for railway track allocation. *OpenAccess Series in Informatics*, 7:62–78, 2007. ISSN 21906807.
- R. Borndörfer, T. Schlechte, and S. Weider. Railway track allocation by rapid branching. *OpenAccess Series in Informatics*, 14(August):13–23, 2010. ISSN 21906807. doi:[10.4230/OASICS.ATMOS.2010.13](https://doi.org/10.4230/OASICS.ATMOS.2010.13).
- U. Brännlund, P. O. Lindberg, A. Nõu, and J. E. Nilsson. Railway timetabling using Lagrangian relaxation. *Transportation Science*, 32(4):358–369, 1998. ISSN 00411655. doi:[10.1287/trsc.32.4.358](https://doi.org/10.1287/trsc.32.4.358).
- C. Bron and J. Kerbosch. Algorithm 457: Finding All Cliques of an Undirected Graph. *Communications of the ACM*, 16(9):575–577, 1973. ISSN 15577317. doi:[10.1145/362342.362367](https://doi.org/10.1145/362342.362367).
- V. Cacchiani, A. Caprara, and P. Toth. A column generation approach to train timetabling on a corridor. *4or*, 6(2):125–142, 2008. ISSN 16142411. doi:[10.1007/s10288-007-0037-5](https://doi.org/10.1007/s10288-007-0037-5).
- V. Cacchiani, A. Caprara, and M. Fischetti. A lagrangian heuristic for robustness, with an application to train timetabling. *Transportation Science*, 46(1):124–133, 2012. ISSN 15265447. doi:[10.1287/trsc.1110.0378](https://doi.org/10.1287/trsc.1110.0378).
- V. Cacchiani, D. Huisman, M. Kidd, L. Kroon, P. Toth, L. Veenturf, and J. Wagenaar. An overview of recovery models and algorithms for real-time railway rescheduling. *Transportation Research Part B: Methodological*, 63:15–37, 2014. ISSN 01912615. doi:[10.1016/j.trb.2014.01.009](https://doi.org/10.1016/j.trb.2014.01.009).
- A. Caprara. Almost 20 Years of Combinatorial Optimization for Railway Planning: from Lagrangian Relaxation to Column Generation. In *10th Workshop on Algorithmic Approaches for Transportation Modelling, Optimization, and Systems (ATMOS'10)*, OpenAccess Series in Informatics (OASICS), 2010.
- A. Caprara, M. Fischetti, and P. Toth. Modeling and solving the train timetabling problem. *Operations Research*, 50(5), 2002. ISSN 0030364X. doi:[10.1287/opre.50.5.851.362](https://doi.org/10.1287/opre.50.5.851.362).
- A. Caprara, M. Monaci, P. Toth, and P. L. Guida. A Lagrangian heuristic algorithm for a real-world train timetabling problem. *Discrete Applied Mathematics*, 154(5 SPEC. ISS.):738–753, 2006. ISSN 0166218X. doi:[10.1016/j.dam.2005.05.026](https://doi.org/10.1016/j.dam.2005.05.026).

- F. Corman, A. D’Ariano, D. Pacciarelli, and M. Pranzo. A tabu search algorithm for rerouting trains during rail operations. *Transportation Research Part B: Methodological*, 44(1):175–192, 2010. ISSN 01912615. doi:[10.1016/j.trb.2009.05.004](https://doi.org/10.1016/j.trb.2009.05.004).
- F. H. W. Dahms, A.-L. Frank, S. Kühn, and D. Pöhle. Transforming Automatic Scheduling in a Working Application for a Railway Infrastructure Manager. *Linköping Electronic Conference Proceedings*, 69(19):280–289, 2019.
- A. D’Ariano, D. Pacciarelli, and M. Pranzo. A branch and bound algorithm for scheduling trains in a railway network. *European Journal of Operational Research*, 183(2):643–657, 2007. ISSN 03772217. doi:[10.1016/j.ejor.2006.10.034](https://doi.org/10.1016/j.ejor.2006.10.034).
- A. D’Ariano, F. Corman, D. Pacciarelli, and M. Pranzo. Reordering and local rerouting strategies to manage train traffic in real time. *Transportation Science*, 42(4):405–419, 2008. ISSN 15265447. doi:[10.1287/trsc.1080.0247](https://doi.org/10.1287/trsc.1080.0247).
- DB. Stammdatenaktualisierung des trassenportals (tpn). URL <https://www.dbinfrago.com/web/aktuelles/kund-inneninformationen/kund-inneninformationen/2023-KW24-Stammdatenaktualisierung-Trassenportal-12390678>. Accessed January 19, 2024.
- G. Desaulniers, J. Desrosiers, and M. Solomon. Strategies for the parallel implementation of metaheuristics. *Operations Research/ Computer Science Interfaces Series*, 15(January 1999):263–308, 1999. ISSN 1387666X. doi:[10.1007/978-1-4615-1507-4](https://doi.org/10.1007/978-1-4615-1507-4).
- J. Desrosiers and M. E. Lübbecke. A Primer in Column Generation. In G. Desaulniers, J. Desrosiers, and M. M. Solomon, editors, *Column Generation*, chapter 1, pages 1–32. Springer New York, NY, 2005. ISBN 978-0-387-25486-9. doi:<https://doi.org/10.1007/b135457>.
- M. E. Dyer and L. A. Wolsey. Formulating the single machine sequencing problem with release dates as a mixed integer program. *Discrete Applied Mathematics*, 26(2-3):255–270, 1990. ISSN 0166218X. doi:[10.1016/0166-218X\(90\)90104-K](https://doi.org/10.1016/0166-218X(90)90104-K).
- W. Fang, S. Yang, and X. Yao. A Survey on Problem Models and Solution Approaches to Rescheduling in Railway Networks. *IEEE Transactions on Intelligent Transportation Systems*, 16(6):2997–3016, 2015. ISSN 15249050. doi:[10.1109/TITS.2015.2446985](https://doi.org/10.1109/TITS.2015.2446985).
- L. Lamorgese and C. Mannino. An exact decomposition approach for the optimal real-time train rescheduling problem. *PATAT 2012 - Proceedings of the 9th International Conference on the Practice and Theory of Automated Timetabling*, (October 2023):428–432, 2012.
- L. Lamorgese, C. Mannino, and M. Piacentini. Optimal train dispatching by Benders’-like reformulation. *Transportation Science*, 50(3):910–925, 2016. ISSN 15265447. doi:[10.1287/trsc.2015.0605](https://doi.org/10.1287/trsc.2015.0605).
- F. Leutwiler and F. Corman. A review of principles and methods to decompose large-scale railway scheduling problems. *EURO Journal on Transportation and Logistics*, 12(December 2021), 2023. ISSN 21924384. doi:[10.1016/j.ejtl.2023.100107](https://doi.org/10.1016/j.ejtl.2023.100107).
- A. Lodi. Mixed Integer Programming Computation. In M. Jünger, D. Naddef, W. R. Pulleyblank, G. Rinaldi, T. M. Liebling, G. L. Nemhauser, G. Reinelt, and L. A. Wolsey, editors, *50 Years of Integer Programming 1958-2008: From the Early Years to the State-of-the-Art*, chapter 16, pages 619–645. 2010. ISBN 9783540682745. doi:[10.1007/978-3-540-68279-0](https://doi.org/10.1007/978-3-540-68279-0).
- M. E. Lübbecke. Column Generation. In *Wiley Encyclopedia of Operations Research and Management Science*. 2011. ISBN 9780470400531. doi:<https://doi.org/10.1002/9780470400531.eorms0158>.
- R. M. Lusby, J. Larsen, M. Ehrgott, and D. M. Ryan. A set packing inspired method for real-time junction train routing. *Computers and Operations Research*, 40(3):713–724, 2013. ISSN 03050548. doi:[10.1016/j.cor.2011.12.004](https://doi.org/10.1016/j.cor.2011.12.004).
- S. J. Maher and E. Rönnberg. Integer programming column generation: accelerating branch-and-price using a novel pricing scheme for finding high-quality solutions in set covering, packing, and partitioning problems. *Mathematical Programming Computation*, 15(3):509–548, 2023. ISSN 18672957. doi:[10.1007/s12532-023-00240-w](https://doi.org/10.1007/s12532-023-00240-w).
- A. Mascis and D. Pacciarelli. Job-shop scheduling with blocking and no-wait constraints. *European Journal of Operational Research*, 143(3):498–517, 2002. ISSN 03772217. doi:[10.1016/S0377-2217\(01\)00338-1](https://doi.org/10.1016/S0377-2217(01)00338-1).
- L. Meng and X. Zhou. Simultaneous train rerouting and rescheduling on an N-track network: A model reformulation with network-based cumulative flow variables. *Transportation Research Part B: Methodological*, 67:208–234, 2014. ISSN 01912615. doi:[10.1016/j.trb.2014.05.005](https://doi.org/10.1016/j.trb.2014.05.005).
- K. Nachtigall and J. Opitz. Modelling and solving a train path assignment model. In M. Lübbecke, A. Koster, P. Letmathe, R. Madlener, B. Peis, and G. Walther, editors, *Operations Research Proceedings 2014*, pages 423–428. Cham, 2016. Springer International Publishing. ISBN 978-3-319-28697-6.
- J. Pachl. *Railway Signalling Principles*. 2 edition, 2021. doi:[10.24355/dbbs.084-202110181429-0](https://doi.org/10.24355/dbbs.084-202110181429-0).

- P. Pellegrini, G. Marlière, and J. Rodriguez. Real time railway traffic management modeling track-circuits. *OpenAccess Series in Informatics*, 25:23–34, 2012. ISSN 21906807. doi:[10.4230/OASIS.ATMOS.2012.23](https://doi.org/10.4230/OASIS.ATMOS.2012.23).
- P. Pellegrini, G. Marlière, and J. Rodriguez. Optimal train routing and scheduling for managing traffic perturbations in complex junctions. *Transportation Research Part B: Methodological*, 59:58–80, 2014. ISSN 01912615. doi:[10.1016/j.trb.2013.10.013](https://doi.org/10.1016/j.trb.2013.10.013).
- P. Pellegrini, G. Marlière, R. Pesenti, and J. Rodriguez. RECIFE-MILP: An Effective MILP-Based Heuristic for the Real-Time Railway Traffic Management Problem. *IEEE Transactions on Intelligent Transportation Systems*, 16(5): 2609–2619, 2015. ISSN 15249050. doi:[10.1109/TITS.2015.2414294](https://doi.org/10.1109/TITS.2015.2414294).
- E. Reynolds and S. J. Maher. A data-driven, variable-speed model for the train timetable rescheduling problem. *Computers and Operations Research*, 142(February 2021):105719, 2022. ISSN 03050548. doi:[10.1016/j.cor.2022.105719](https://doi.org/10.1016/j.cor.2022.105719).
- E. Reynolds, M. Ehrgott, S. J. Maher, A. Patman, and J. Y. T. Wang. A multicommodity flow model for rerouting and retiming trains in real-time to reduce reactionary delay in complex station areas. *Optimization Online*, pages 1–37, 2020.
- M. Samà, A. D’Ariano, F. Corman, and D. Pacciarelli. A variable neighbourhood search for fast train scheduling and routing during disturbed railway traffic situations. *Computers and Operations Research*, 78:480–499, 2017. ISSN 03050548. doi:[10.1016/j.cor.2016.02.008](https://doi.org/10.1016/j.cor.2016.02.008).
- W. Schwanhäüßer. *Die Bemessung der Pufferzeiten im Fahrplangefüge der Eisenbahn*. doctoral dissertation, Fakultät für Bauwesen der Rheinisch-Westfälischen Technischen Hochschule Aachen, 1974.
- E. Tomita. Efficient Algorithms for Finding Maximum and Maximal Cliques and Their Applications. In S. H. Poon, M. S. Rahman, and H. C. Yen, editors, *WALCOM: Algorithms and Computation*, pages 3–15, 2017. ISBN 9783319539249. doi:[10.1007/978-3-319-53925-6](https://doi.org/10.1007/978-3-319-53925-6).
- VIA-Con. About luks. URL <https://www.via-con.de/en/about-luks/>. Accessed December 13, 2023.